Sounding the time Unwinding of the PRoton-to-Electron Mass ratiO

SUPREMO

INFN CSN2 – NA & FI

Resp. Naz. (NA): P. Maddaloni

Resp. FI: P. De Natale

Istituto Nazionale di Fisica Nucleare

Consiglio Nazionale delle Ricerche

Main Goal

Constrain over a-few-year timescale the fractional temporal variation of the proton-to-electron mass ratio, $\beta = m_p / m_e$, at a level of 10^{-15}/yr by means of a spectroscopic frequency measurement on a beam of cold and slow molecules

Transition		Energy scaling
Atomic	Gross structure	Ry
	Fine structure	$\alpha^2 Ry$
	Hyperfine structure	$\alpha^2(\mu/\mu_B)Ry$
Molecular	Electronic structure	Ry
	Vibrational structure	$\beta^{-1/2}Ry$
	Rotational structure	$\beta^{-1}Ry$
Relativistic corrections		Function of α

Possible validation of modern MD (string-type) theories seeking to unify the four known fundamental interactions; reconstruction of the dark-energy equation of state

📖 C. Kiefer, Lect. Notes Phys. **648**, 115 (2004)

📖 P.P. Avelino et al., Phys. Rev. D **74**, 083508 (2006)

Measure the frequency of a molecular ro-vibrational transition relative to the Cs clock hyperfine transition

$$\frac{1}{\frac{\nu(M)}{\nu(Cs)}}\frac{\partial\left[\frac{\nu(M)}{\nu(Cs)}\right]}{\partial t} = -\frac{1}{2\beta}\frac{\partial\beta}{\partial t} - 2.83\frac{1}{\alpha}\frac{\partial\alpha}{\partial t} - \frac{1}{\frac{\mu_{Cs}}{\mu_B}}\frac{\partial\left(\frac{\mu_{Cs}}{\mu_B}\right)}{\partial t}$$

where limits on α and μ_{Cs}/μ_B are inferred from atomic-clock measurements

📖 R.M. Godun et al., Phys. Rev. Lett. **113**, 210801 (2014)

📖 N. Huntemann et al., Phys. Rev. Lett. **113**, 210802 (2014)

Three target molecules with associated experimental strategies are identified

acetylene, fluoroform (NA)

carbon monoxide (FI)

Direct cooling of ground-state molecules

Buffer gas cooling

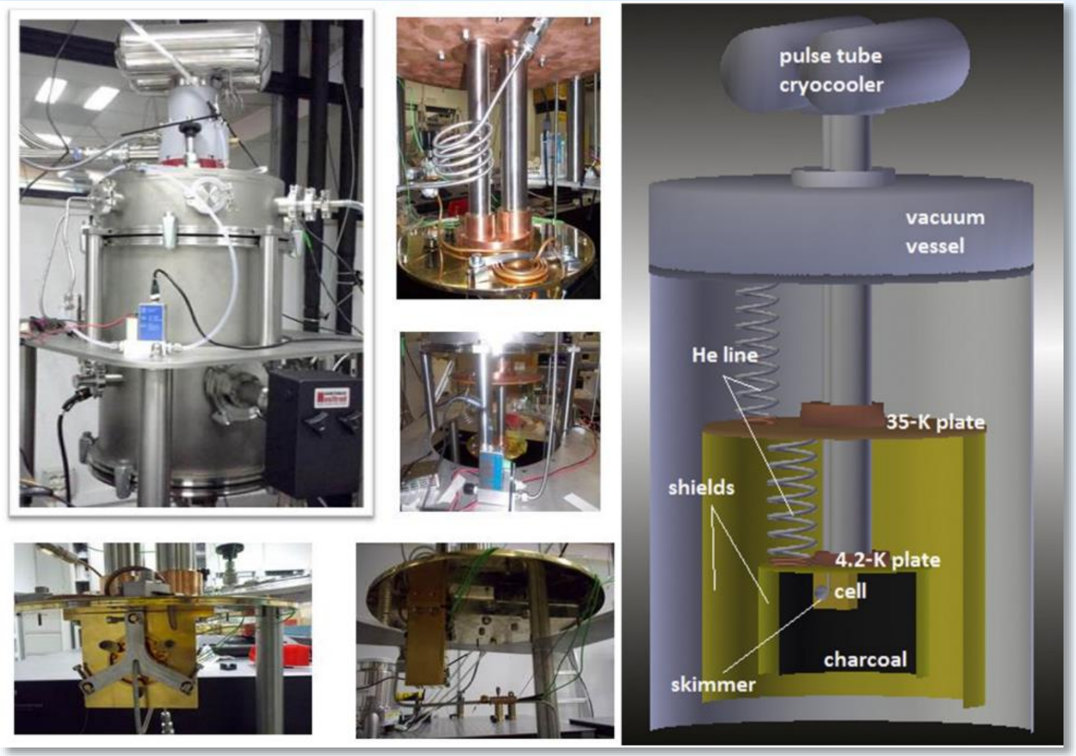

Both translational and rotational degrees of freedom of the desired species are cooled via collisions with a thermal bath of helium in a cryogenic cell that is in contact with the cold plate of a pulse-tube cryocooler; then, a molecular beam is formed by expansion in a high vacuum, typically in the partially-hydrodynamic regime.

Stark deceleration

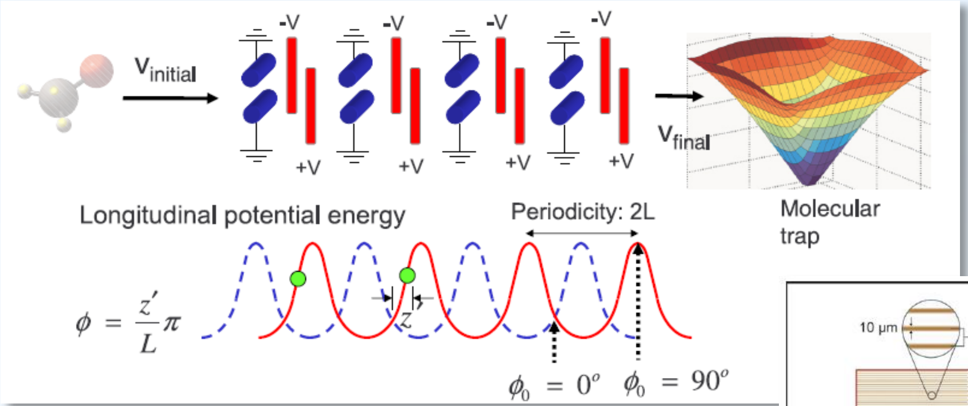

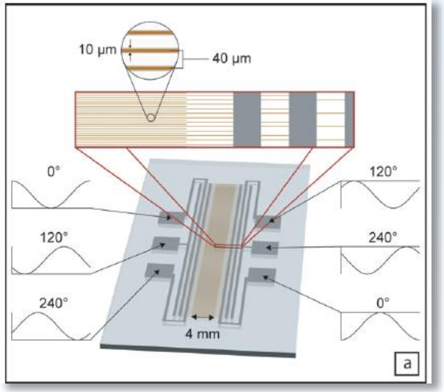

The molecular dipole moment interacts with a properly generated time-varying electric field gradient → loss of kinetic energy is due to the coerced gain of Stark potential (Sisyphus-type scheme).

Symphatetic cooling

W.G. Rellergert et al., Nature **495**, 490 (2013)

The vibrational motion of trapped $BaCl^+$ molecules is quenched by collisions with ultra-cold calcium atoms at a rate that is over four orders of magnitude more efficient than traditional sympathetic cooling schemes

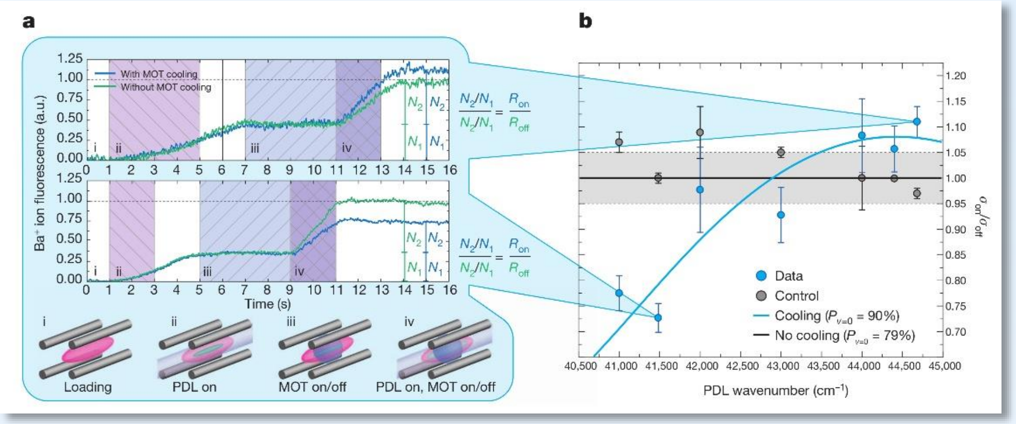

Magneto-optical trapping

J.F. Barry et al., Nature **512**, 286 (2014)

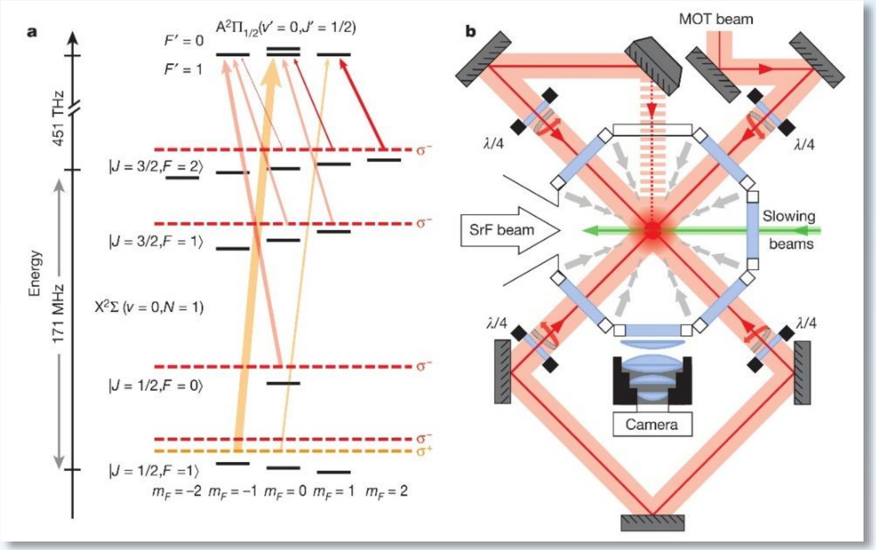

3D MOT of SrF at a temperature of ~ 2 mK, loaded with pulses from a cryogenic buffer gas beam source that have been slowed using radiation pressure

Evaporative cooling

B.K. Stuhl et al., Nature 492, 396 (2012)

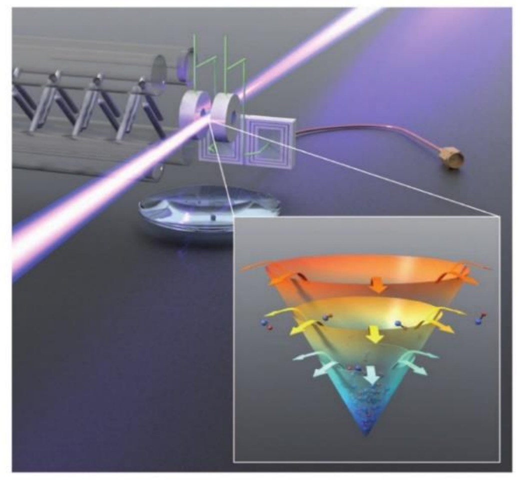

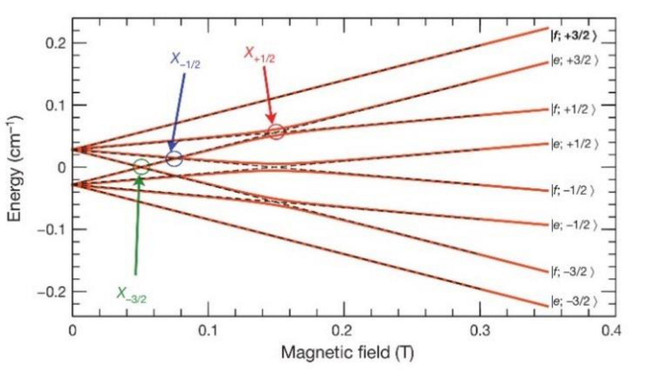

Microwave forced evaporative cooling of neutral hydroxyl molecules loaded from a Stark-decelerated beam into a magnetic quadrupole trap

CRDS of buffer-gas-cooled acetylene

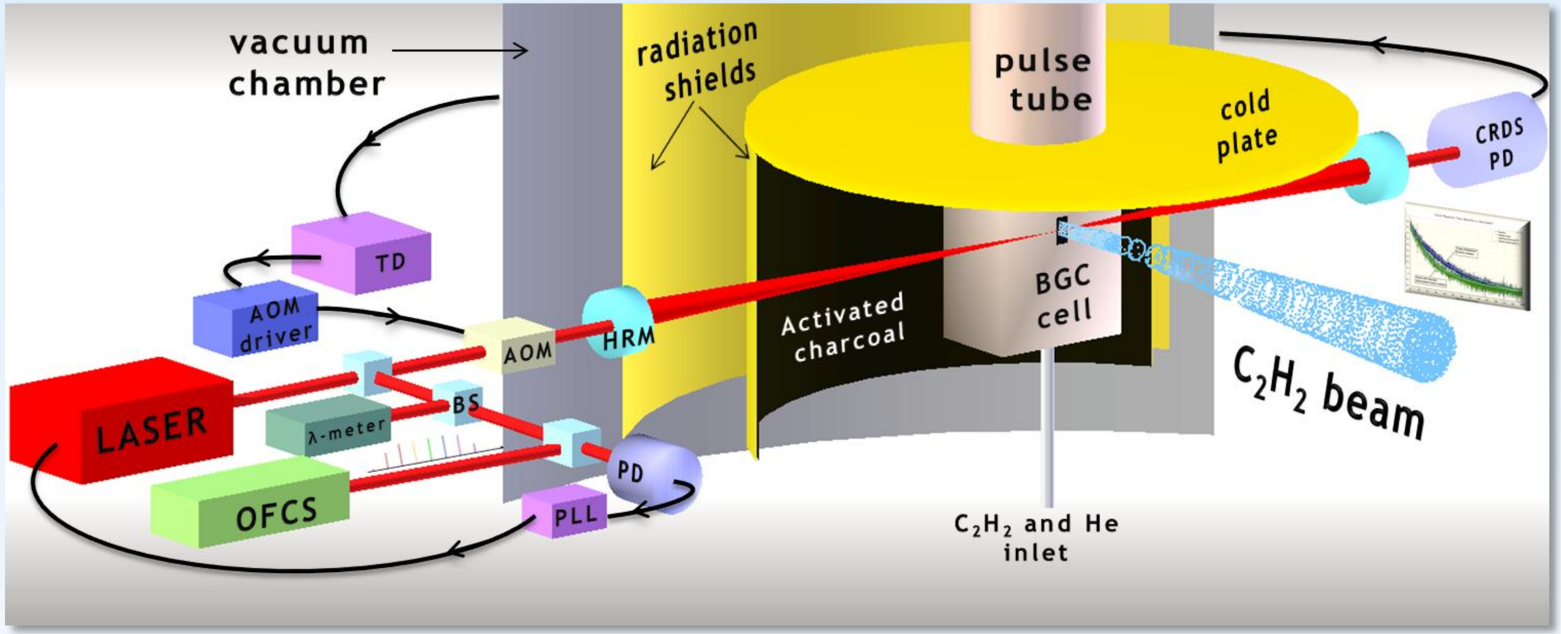

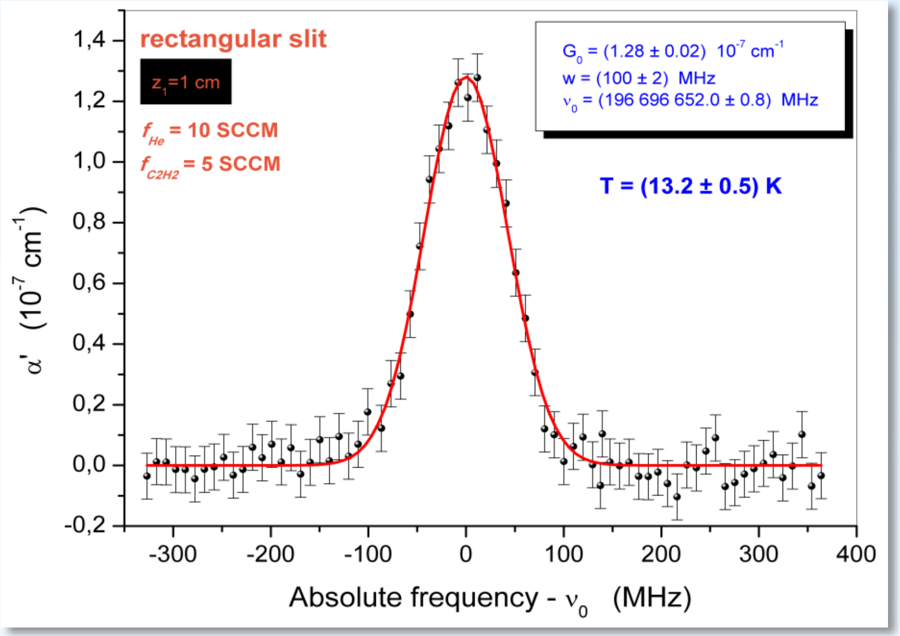

$$G(\nu) = G_0 \exp\left[-\frac{4\ \ln 2(\nu-\nu_0)^2}{w^2}\right]$$

$$w = \frac{\nu_0}{c}\sqrt{\frac{8\ \ln 2\, k_B T}{m}}$$

$$\overline{v}_z \simeq 1.4\sqrt{\frac{8k_B T}{\pi m_{He}}}\sqrt{1-4\mathrm{Rey}^{-4/5}}$$

$$\mathrm{Rey} \simeq \frac{4f_{He}\sigma_{He-He}}{a_x}\sqrt{\frac{\pi m_{He}}{k_B T}}$$

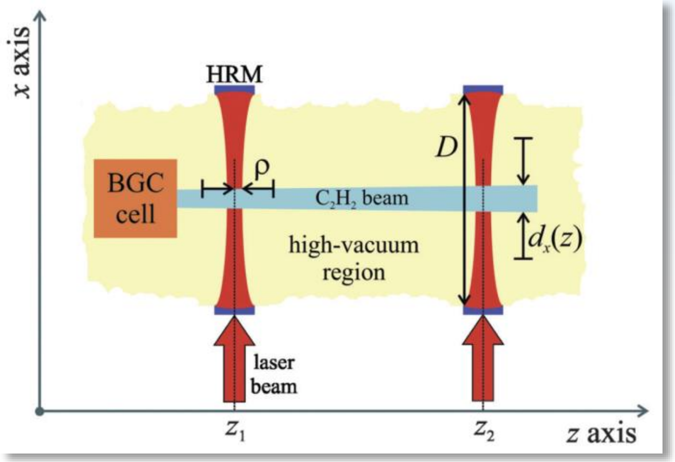

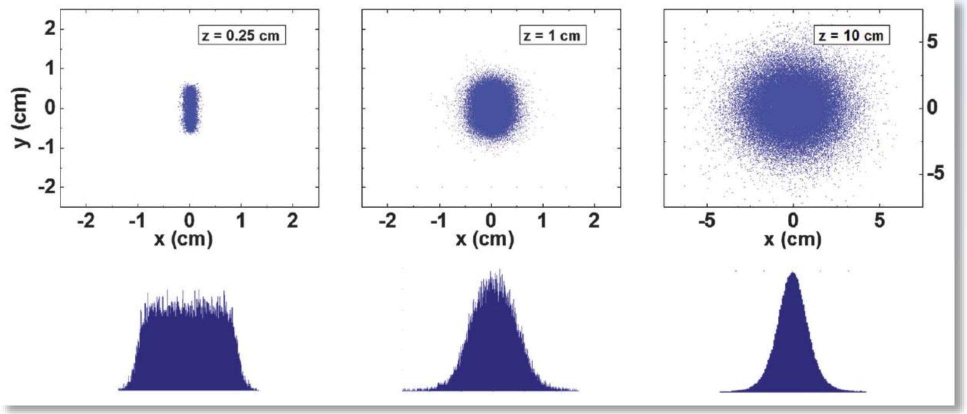

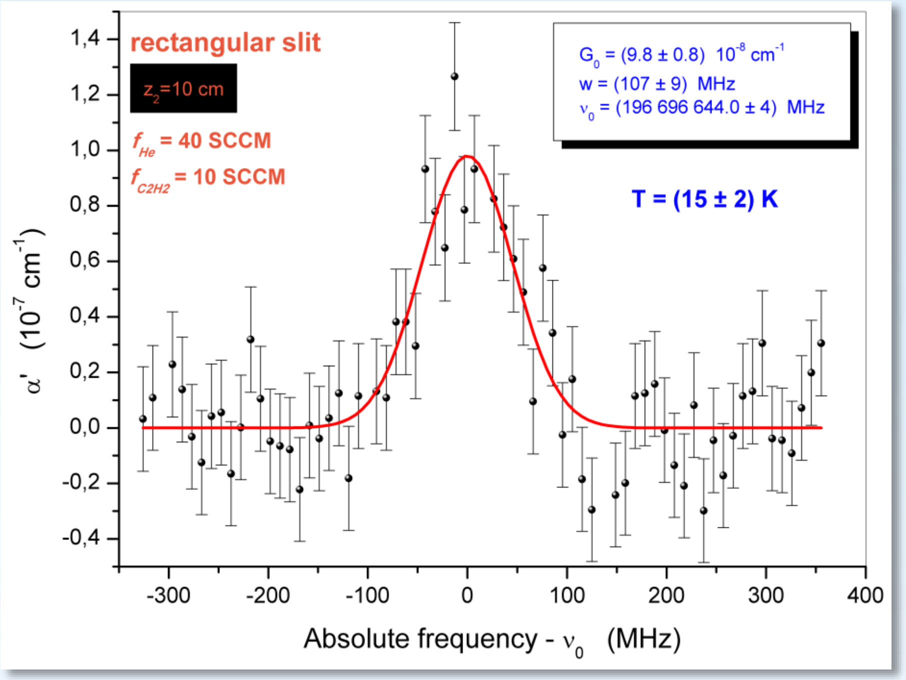

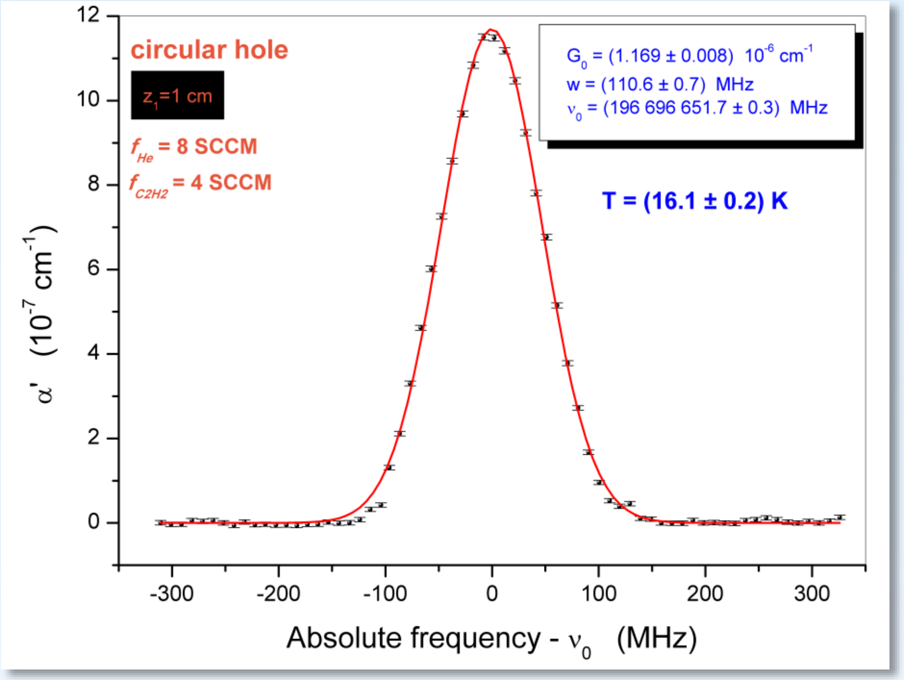

- ✓ **Current beam parameters:**
  $T \approx 15$ K
  Flux $\approx 7 \cdot 10^{14}$ molec/s
  $\bar{v}_z \approx 340$ m/s
  $\Delta\theta \approx 23^{\circ}$

- ✓ **The center frequency of the $g \rightarrow (v_1 + v_3)$ R(1) line is measured with an uncertainty of 330 kHz ($1.5 \cdot 10^{-9}$)**

- ➢ Optimization of the beam properties **by lowering the input gas fluxes**, and hence the beam longitudinal speed, in conjunction with an improvement of the cryogenic apparatus intended to preserve the present flux while further reducing temperature.

- ➢ Implementation of two-photon (two-color) spectroscopy

$$\Gamma = \Gamma_{21} + \left|\frac{k_2 - k_1}{k_1}\right| \Gamma_{10}$$

$$S \sim \left(\frac{\mu_{21}\mu_{10}}{\delta} I_{laser}\right)^2$$

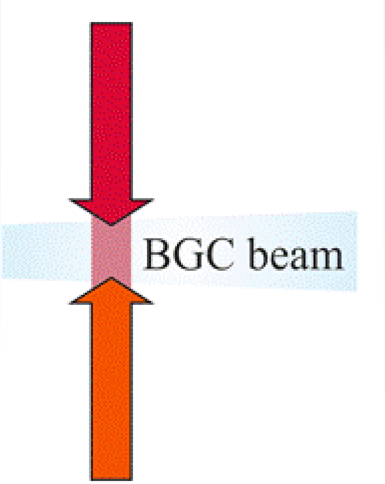

Sub-Doppler gas-cell spectroscopy of CHF_3

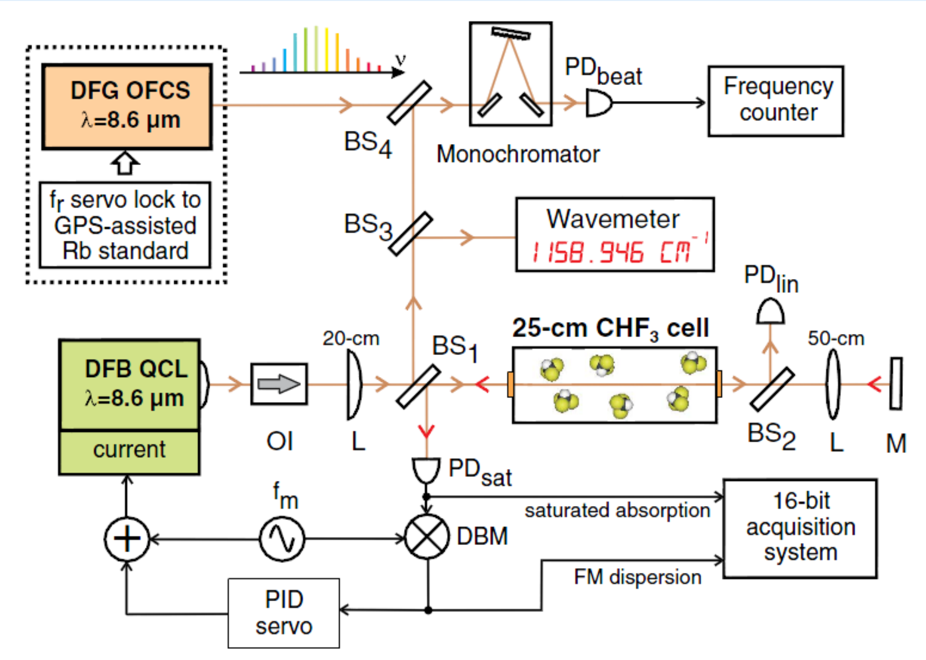

Parameter	Coefficient	Type B Uncertainty (kHz)
CHF_3 pressure, p_{CHF_3}	22(1) kHz/Pa	0.75
Gas cell leakage, p_{leak}	38(2) kHz/Pa	1.5
Laser power, P_{QCL}	45 kHz/mW	0.2
Modulation frequency, f_m	100 Hz/kHz	Negligible
Modulation depth, a_m	16 kHz/MHz	Negligible
Electronic offset	0.3 kHz/mV	0.2
Etalon/interference effects		0.5
Rb-GPS clock		0.04
Total type B uncertainty		1.8 $(5 \cdot 10^{-11})$

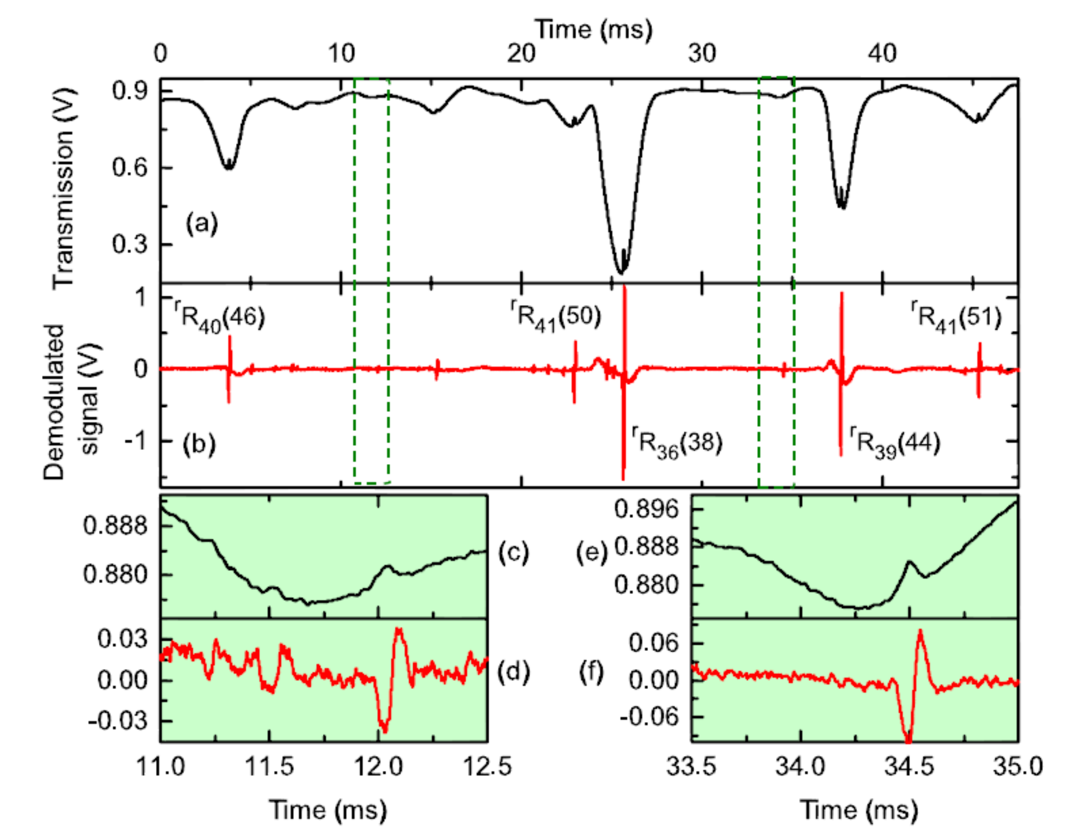

POLITECNICO
MILANO 1863

Fractional frequency precision $8.6 \cdot 10^{-12}$ (1-s integration time), limited by the Rb-clock stability

REMPI spectroscopy of Stark-decelerated CO

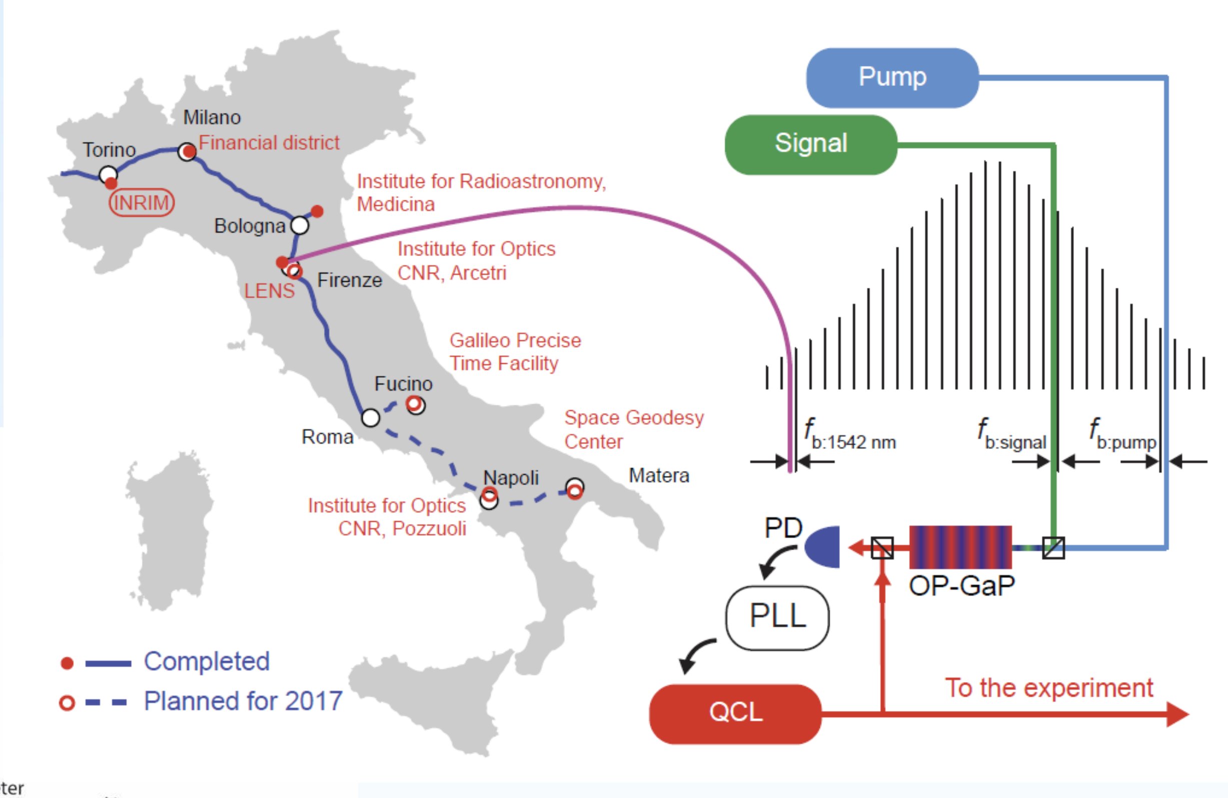

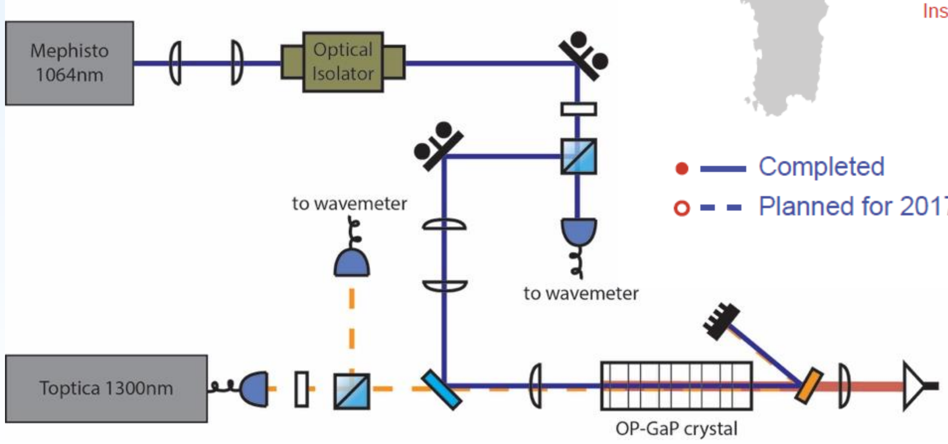

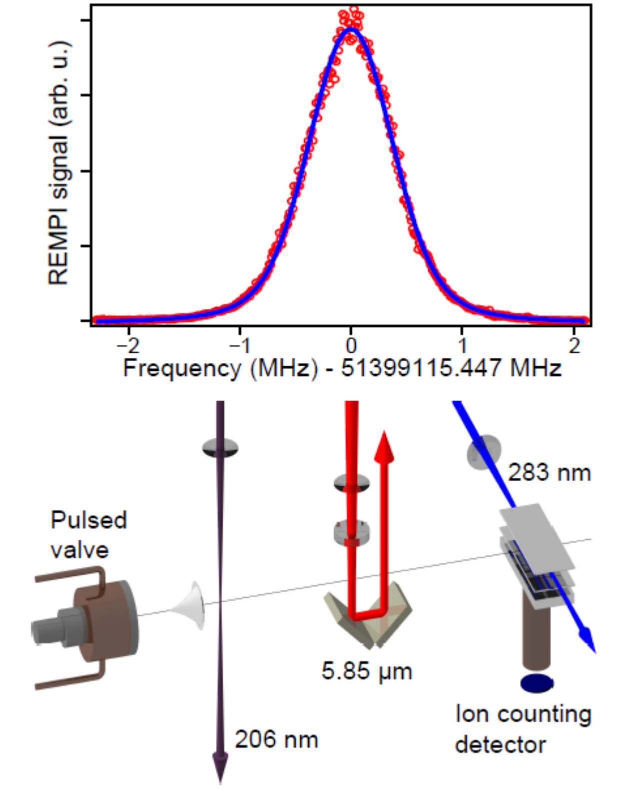

FIG. 3. Top: a typical vibrational absorption spectrum on the $a^3\Pi_1$ metastable state of CO measured in about 20 minutes. The transition $|v = 0, J = 1, + >\leftarrow |v = 1, J = 1, - >$ shows a width of 900 kHz. Bottom: sketch of the molecular beam apparatus used for the measurement. The beam is generated by a pulsed valve operated at 10 Hz. CO molecules are skimmed, excited into the metastable state by a UV laser at 206 nm, interact with the mid IR laser, and are finally detected by resonance-enhanced multiphoton ionization. Ions are collected on a microchannel plates detector.

total statistical uncertainty ≈ 1.7 kHz

Towards two-photon spectroscopy

$^{13}C^{12}CH_2$

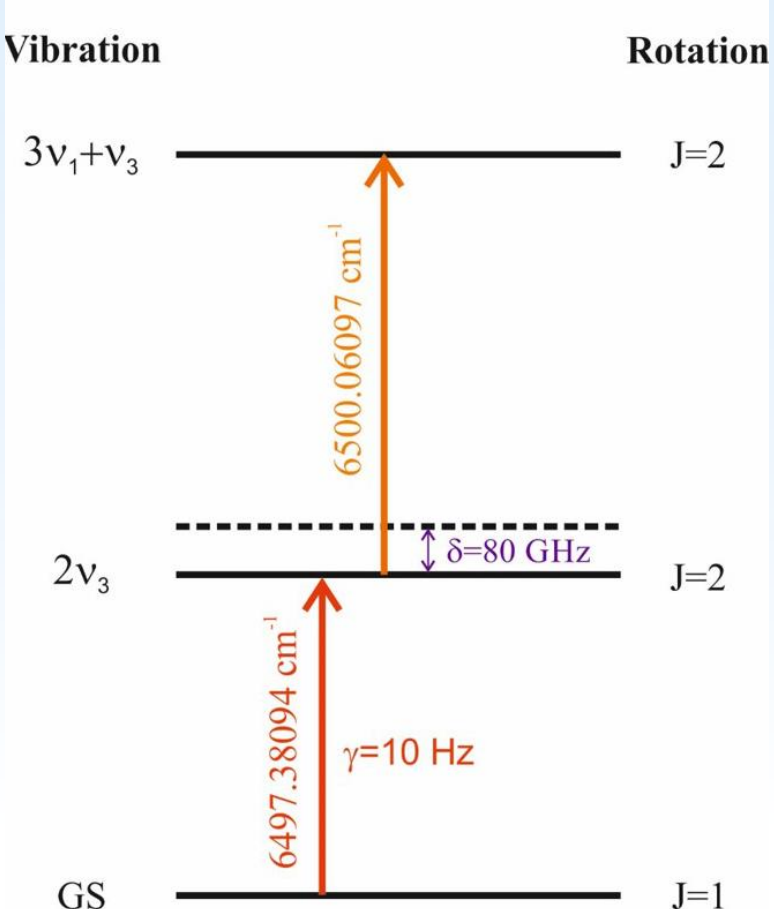

CHF_3

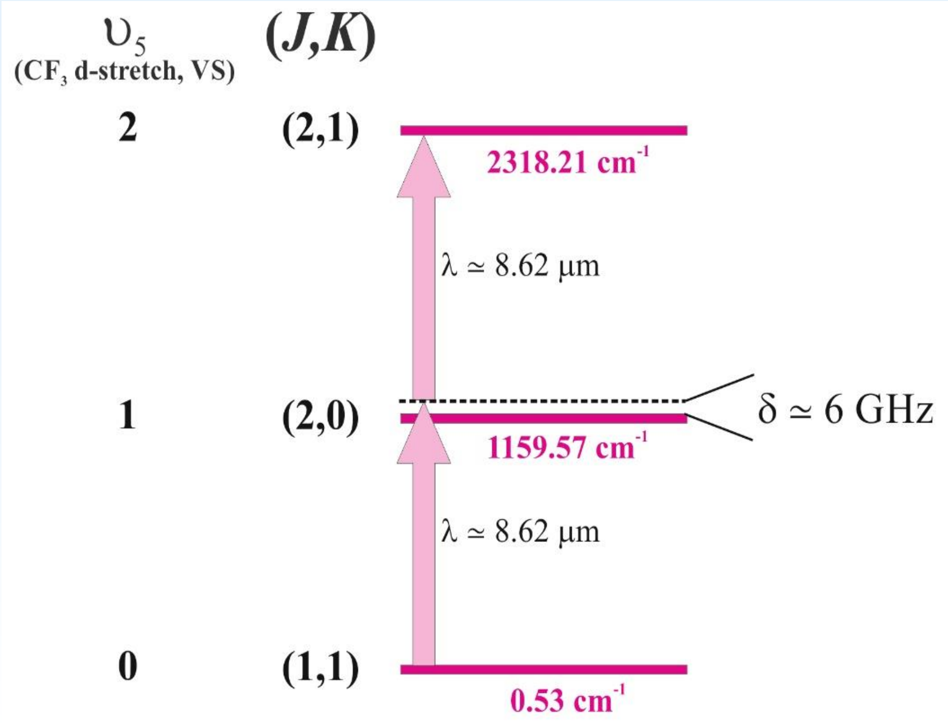

CO

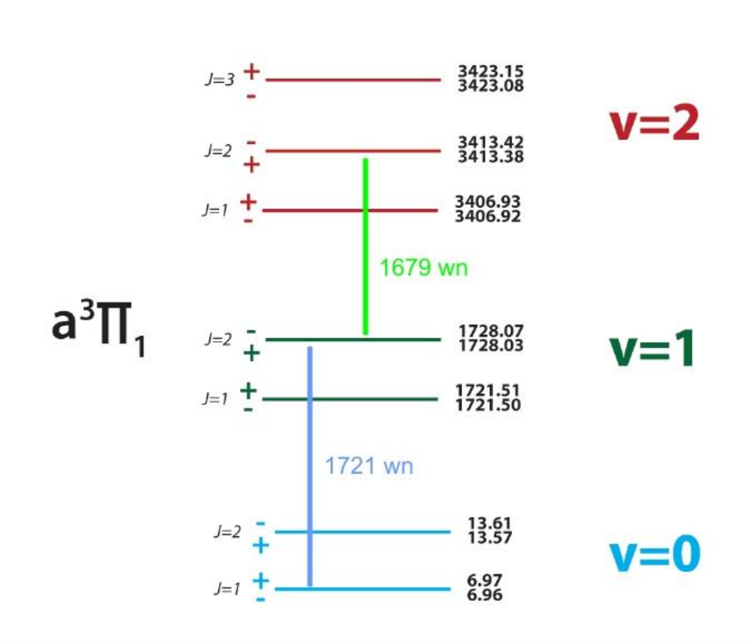

Setup under construction

Enhance the spectroscopic interrogation time by exciting 2-photon Ramsey fringes

$$\mathcal{S}(\omega,T) \sim p_0(T)\left[\frac{\mu_{21}\mu_{10}I_L}{\delta}\frac{d}{u}\right]^2 \int_0^\infty \left[1 + e^{-2\gamma\frac{D}{u}} + 2e^{-\gamma\frac{D}{u}}\cos\frac{(2\omega-\omega_{20})D}{u}\right]\mathcal{F}(\Delta u)\,du$$

Decrease fringe periodicity & increase fringe contrast by using a beam of slow, translationally and rotationally cold molecules

The cold molecular beam is extracted from a buffer-gas-cooling source and then subjected to a 2-photon Ramsey interrogation; the probe laser source is phase-locked to an optical frequency comb (OFC) that is ultimately referenced to the Cs primary standard via the clock laser delivered by National Optical Fiber Link.

$$\mathcal{P} = \frac{u}{2D} = 100\ \text{Hz}$$

$$SNR = 20,\ N_{avg} = 100$$

$$\mathcal{R} \sim \frac{\mathcal{P}}{SNR \cdot \sqrt{N_{avg}}} \sim 500\ \text{mHz}$$

$$\boldsymbol{\mathcal{R}_{frac} \sim 5 \cdot 10^{-15}}$$

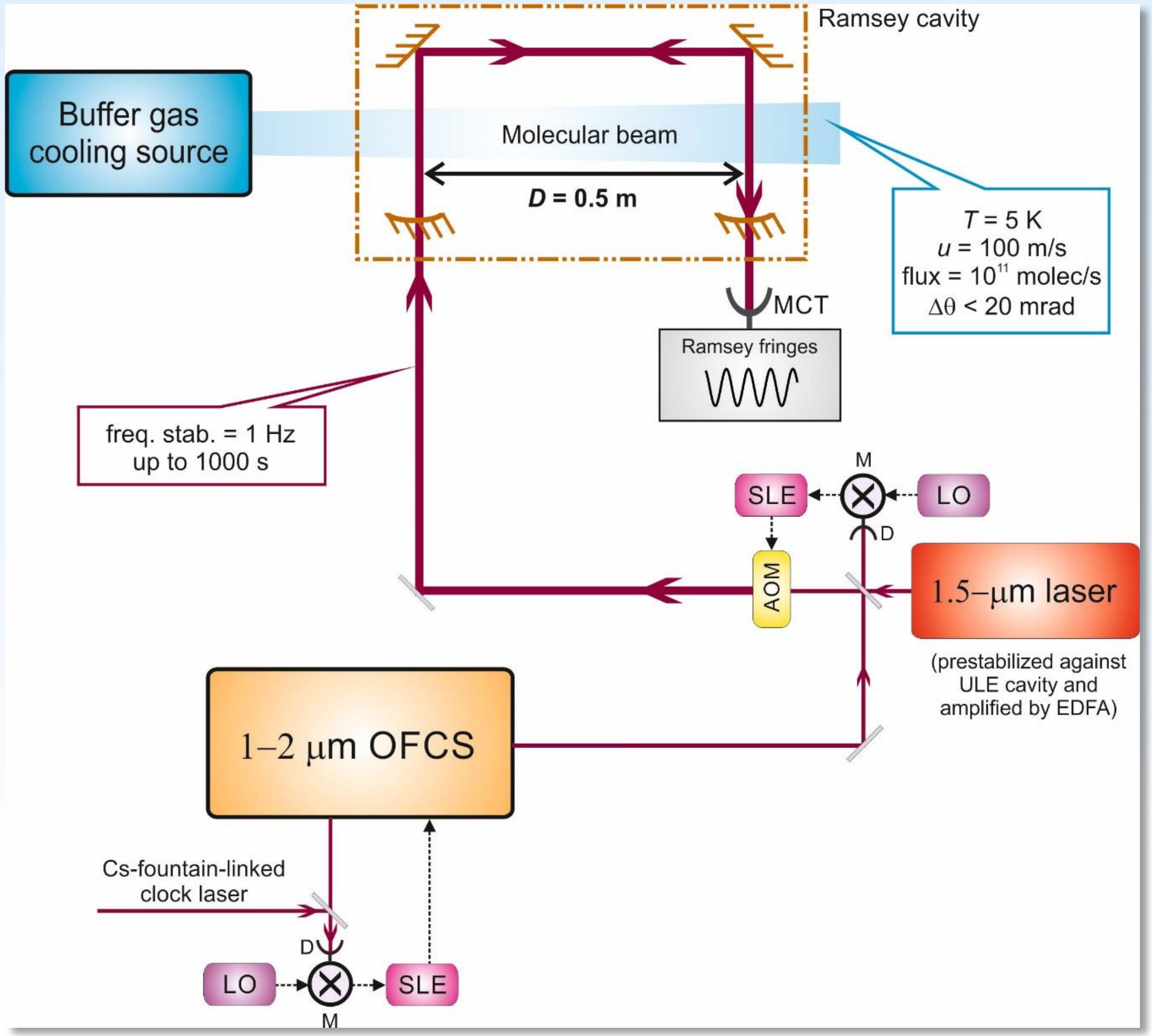

National optical fiber link

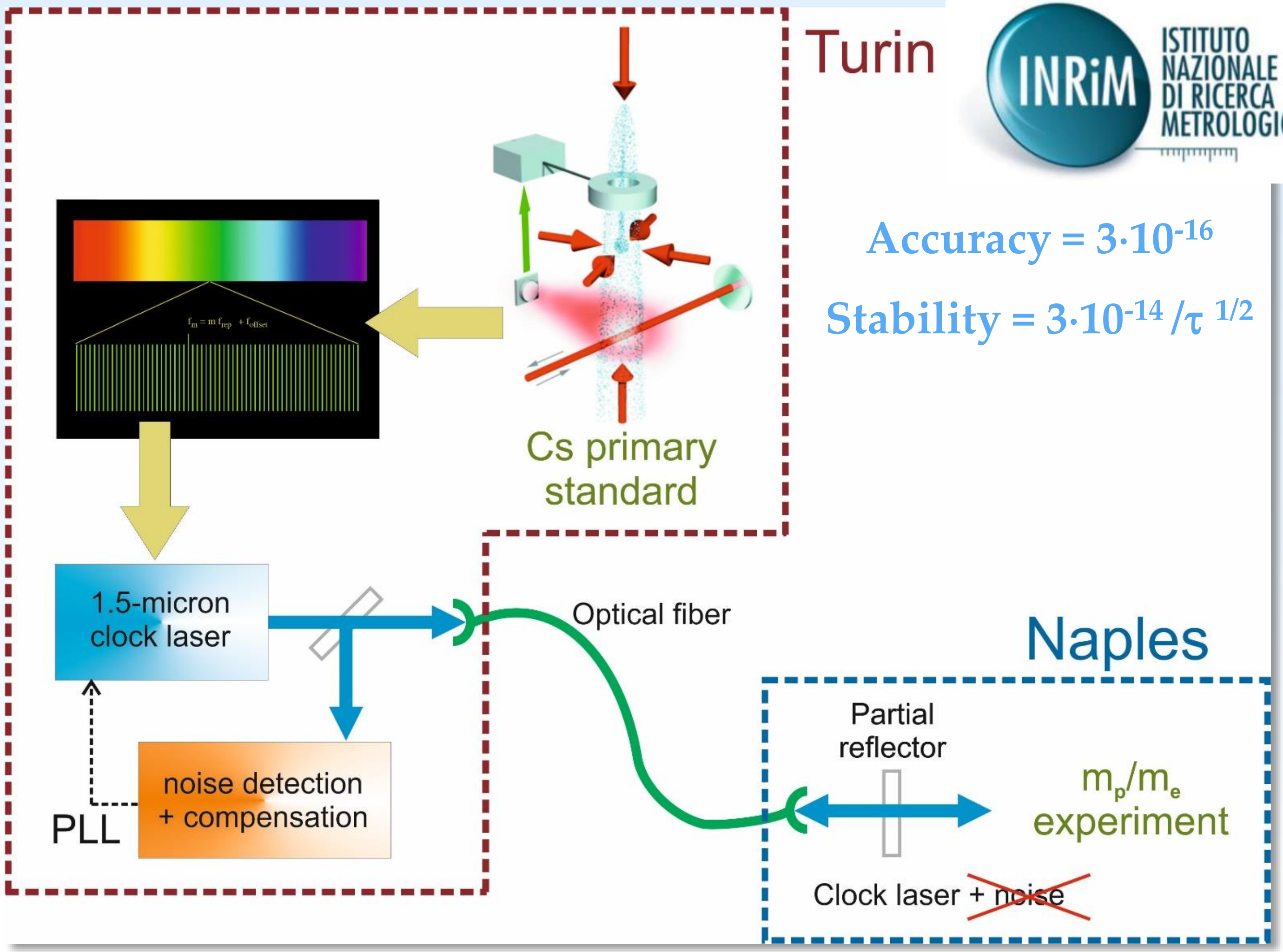

Accuracy = $3 \cdot 10^{-16}$

Stability = $3 \cdot 10^{-14} / \tau^{1/2}$

📖 D. Calonico et al., Appl. Phys. B **117**, 979 (2014)

A 1.5-micron laser, continuosly referenced to the primary Cs fountain via an OFC, is disseminated through a long optical fiber. Part of the laser radiation is reflected back and used to cancel the phase noise accumulated during the fiber propagation

Pushing the ultimate resolution in the spectroscopic frequency measurement down to 10^{-17} by stabilizing the frequency comb, to which the probe laser is referenced, against an optical atomic standard

→ Yb lattice clock under test at INRIM

$$\frac{1}{\frac{\nu_{vib}(M)}{\nu_{el}(Yb)}} \frac{\partial \left[\frac{\nu_{vib}(M)}{\nu_{el}(Yb)}\right]}{\partial t} = -0.5\frac{\dot{\beta}}{\beta} - N_{Yb}\frac{\dot{\alpha}}{\alpha}$$

The *Quantum Manifesto* in the background

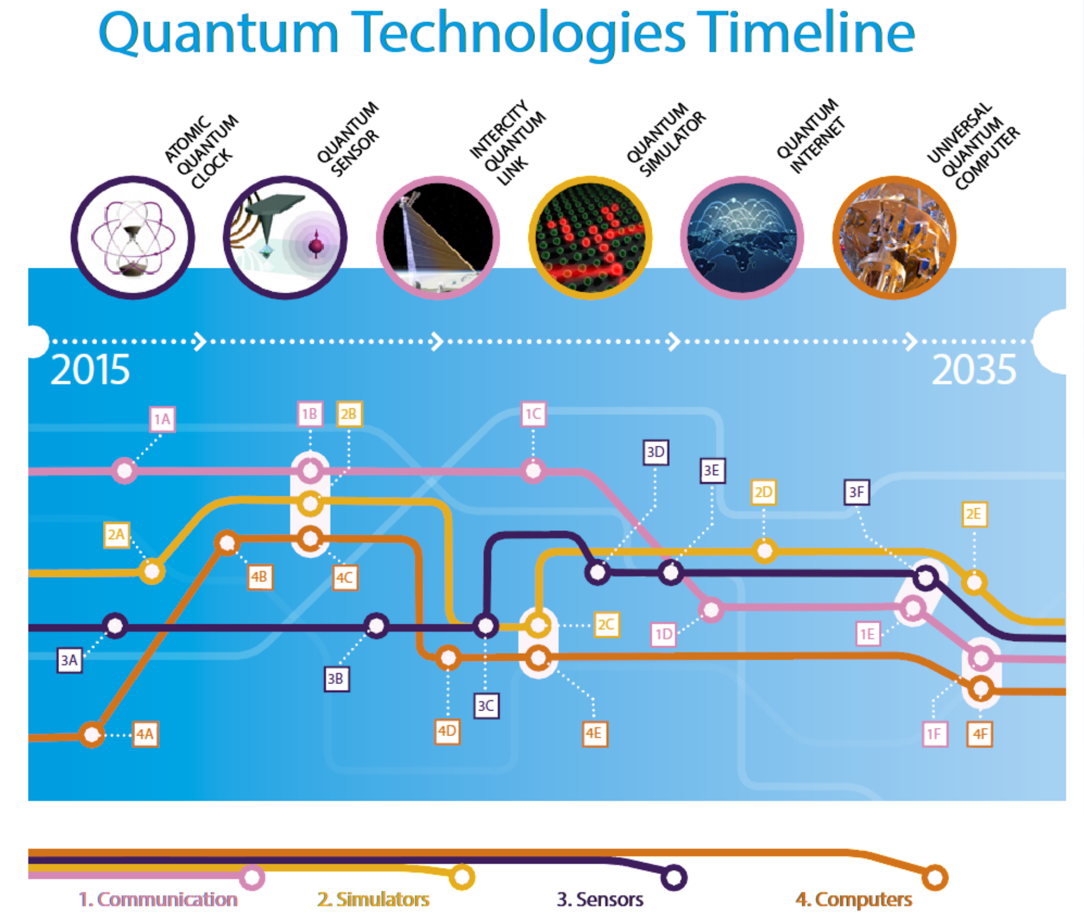

Quantum magnetism with symmetric top molecules

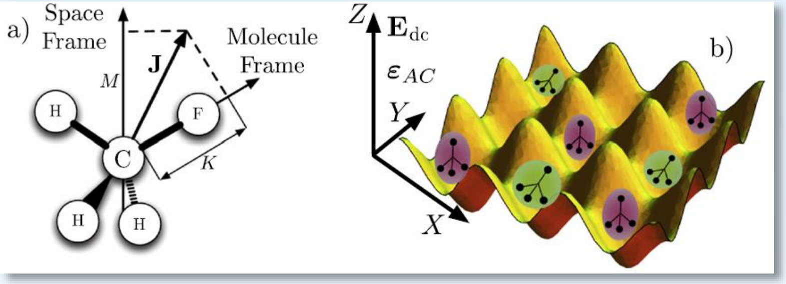

📖 M.L. Wall et al., New. J. Phys. 17, 025001 (2015)

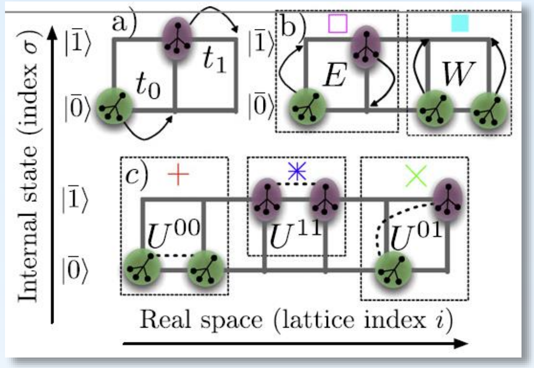

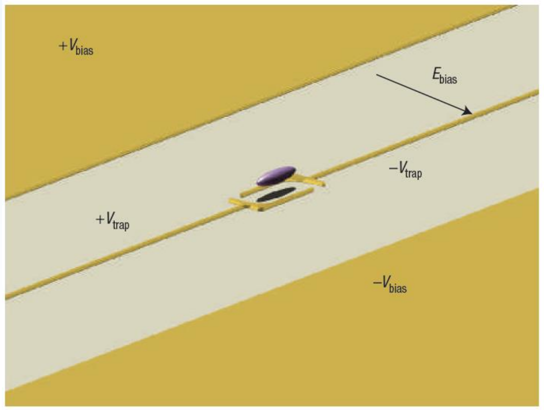

A scalable quantum processor based on a coherent all-electrical interface between polar molecules and a mesoscopic superconducting resonator

📖 A. André et al., Nature Phys. 2, 636 (2006)

Publications 2014-2017

G. Insero, S. Borri, D. Calonico, P. Cancio Pastor, C. Clivati, D. D'Ambrosio1, P. De Natale, M. Inguscio, F. Levi, and G. Santambrogio
Measuring molecular frequencies in the 1-10 m range at 11-digits accuracy
arXiv:1703.10975

Gambetta, E. Vicentini, Y. Wang, N. Coluccelli, E. Fasci, L. Gianfrani, A. Castrillo, V. Di Sarno, L. Santamaria, P. Maddaloni, P. De Natale, P. Laporta, G. Galzerano
Absolute frequency measurements of CHF3 Doppler-free ro-vibrational transitions at 8.6 μm
Opt. Lett. 42, 1911 (2017)

P. Maddaloni, S. Bartalini, P. Cancio, M. De Rosa, D. Mazzotti, P. De Natale
Frontiers of molecular gas sensing
Rivista del Nuovo Cimento 40, 135 (2017)

M. Siciliani de Cumis, S. Borri, G. Insero, I. Galli, A. Savchenkov, D. Eliyahu, V. Ilchenko, N. Akikusa, A. Matsko, L. Maleki, and P. De Natale
Microcavity-Stabilized Quantum Cascade Laser
Laser Photonics Rev. 10, 153 (2016)

S. Borri, M. Siciliani de Cumis, G. Insero, S. Bartalini, P. Cancio, D. Mazzotti, I. Galli, G. Giusfredi, G. Santambrogio, A. Savchenkov, D. Eliyahu, V. Ilchenko, N. Akikusa, A. Matsko, L. Maleki, and P. De Natale
Tunable Microcavity-Stabilized quantum cascade laser for Mid-IR High-Resolution spectroscopy and sensing
Sensors 16, 238 (2016)

G. Insero, C. Clivati, D. D'Ambrosio, P. De Natale, G. Santambrogio, P. G. Schunemann, J. J. Zondy, and S. Borri
Difference frequency generation in the mid-infrared with orientation-patterned gallium phosphide crystals
Opt. Lett. 41, 5114 (2016)

L. Santamaria, V. Di Sarno, P. De Natale, M. De Rosa, M. Inguscio, S. Mosca, I. Ricciardi, D. Calonico, F. Levi, P. Maddaloni
Comb-assisted cavity ring-down spectroscopy of a buffer-gas-cooled molecular beam
Physical Chemistry Chemical Physics 18, 16715 (2016)

A. Gambetta, N. Coluccelli, M. Cassinerio, T. T. Fernandez, D. Gatti, A. Castrillo, E. Fasci, L. Gianfrani, L. Santamaria, V. Di Sarno, P. Maddaloni, P. De Natale, P. Laporta, G. Galzerano
Frequency-comb-assisted precision laser spectroscopy of CHF3 around 8.6 μm
The Journal of Chemical Physics 143, 234202 (2015)

L. Santamaria, C. Braggio, G. Carugno, V. Di Sarno, P. Maddaloni, G. Ruoso
Axion dark matter detection by laser spectroscopy of ultracold molecular oxygen: a proposal
New Journal of Physics 17, 113025 (2015)

L. Santamaria, V. Di Sarno, I. Ricciardi, M. De Rosa, S. Mosca, P. Maddaloni, P. De Natale
Low-temperature spectroscopy of the 12C2H2 (v1+v3) band in a helium buffer gas
The Astrophysical Journal 801, 50 (2015)

L. Santamaria, V. Di Sarno, I. Ricciardi, S. Mosca, M. De Rosa, P. Maddaloni, P. De Natale
Assessing the time constancy of the proton-to-electron mass ratio by precision ro-vibrational spectroscopy of a cold molecular beam
Journal of Molecular Spectroscopy 300, 116 (2014)